

Research on Defect Detection of Oil and Gas Pipeline Based on Far - Field Eddy Current Technology

Hao Wen, Mingjiang Shi

Southwest Petroleum University, Chengdu, 610500, China

Abstract

As oil and natural gas contain a lot of corrosive components during gathering process, they will cause corrosion, such as perforation and grooves, etc., so as to ensure the safety of gathering pipelines, it is necessary to detect corrosion defects. The remote field eddy current (RFFC) technology has applied to simulate and study the corrosion defect detection of pipeline, and the relationship between the defect depth of the pipeline and the corresponding detection signal is obtained.

Keywords

Oil and gas gathering pipeline; Pipeline defect; remote field eddy current (RFFC); Magnetic induction.

1. Introduction

Oil and gas often contain large quantities of components that can corrode pipes during the collection and transportation. Over time, the internal and external walls of the gathering and transporting pipelines will be corroded by a large number of defects, seriously affecting the normal operation of the entire oilfield. Regular detection of corrosion defects in the oil gathering pipelines can effectively prevent oilfield safety accidents caused by pipe breakage.

Far-field eddy current technology has a small lift-off effect, the detection sensitivity of the inner and outer wall of the pipe is consistent, the detection result is less related to the displacement of the probe and other characteristics are widely used in heat exchanger tubes and other small diameter defects detection , For oil and gas pipelines, due to the larger diameter and wall thickness, resulting in lower sensitivity applications are limited[1]. Based on the conventional far-field eddy current probe structure, the detection coil is designed as a number of small detection coils, and the differential structure is adopted to reduce the interference. The feasibility of the scheme is verified through simulation analysis and experimental study.

2. Far-field eddy current detection technology principles

The far-field eddy current testing technology uses the built-in probe to detect the pipe wall defect information, which is a low-frequency eddy current testing technology that penetrates the metal pipe wall[2]. Detection principle shown in Figure 1, including the excitation coil in the coaxial position of the pipe, the detection coil far field.

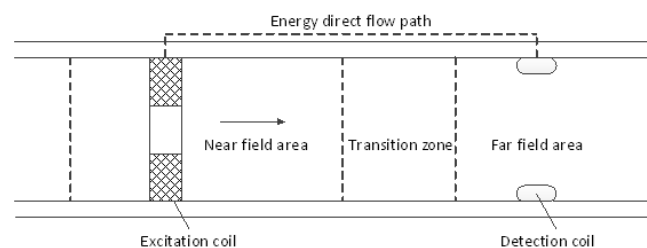


Fig.1 Far-field eddy current probe structure diagram

When the excitation coil is fed with a sinusoidal alternating current of low frequency, three typical far-field vortex phenomena in the near-field, transition and far-field regions are formed in the tube, and a direct energy flow path emerges in the tube, near the outer wall of the tube Energy indirect flow path[3].

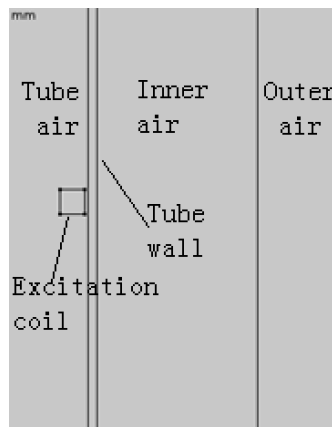


Fig.2 Far-Field Eddy Simulation Model

In the near-field region (1.8 times the inner diameter of the tube), the excitation coil produces the most intense alternating magnetic field, but with increasing axial distance from the excitation coil, due to the shielding effect of induced vortices in the tube wall near the excitation coil, The intensity will rapidly decay to a minimum, the magnetic field distribution in this region can not contribute to the defect detection signal[4-5]; the significance of the defect recognition is far field (about 3 times the tube diameter), the excitation coil and its adjacent tube The wall constitutes a transformer structure that generates a circumferential vortex within the tube wall, a portion of which rapidly diffuses to the outer surface of the tube, which in turn causes the alternating magnetic field to diffuse into the air outside the tube wall and conduct along the tube until In the far field, the energy in the far field is much larger than the direct energy. Therefore, the magnetic field outside the tube passes through the wall again and enters the far field. The magnetic fields in the far field passing through the two walls of the tube contain information of wall defects and can be detected by the detection coil Identify and identify defects[6].

3. Simulation of far field vortex flow in pipelines

3.1 Establishment of far-field eddy simulation model

For the basic phenomenon of far-field eddy current and full circumferential defects For finite element simulation of detection, since the model is completely axisymmetric, it is only necessary to establish a two-dimensional axisymmetric model analysis. The simulation model is shown in Fig.2.

The model is horizontal for the r-axis, vertical z-axis. The excitation coil has an outer diameter of 94 mm, an inner diameter of 64 mm and a length of 15 mm, a relative permeability of 1, an electrical conductivity of $3.33 \times 10^7 \text{ S/m}$, and a number of turns of the coil of 350; a ferromagnetic wall thickness of 5 mm; an inner diameter of 98 mm; , Length 1600mm, relative permeability of 129.5, conductivity of $5.9 \times 10^6 \text{ S/m}$; boundary layer between the outer air and inner air space at $r = 150 \text{ mm}$ Department, and the application of grid control virtual operation.

3.2 No Defect Simulation of Far Field Eddy Current

To the excitation coil current density of $6.2 \times 10^6 \text{ A/m}^2$, the frequency of 70Hz excitation conditions, the distribution of magnetic lines shown in Figure 3.

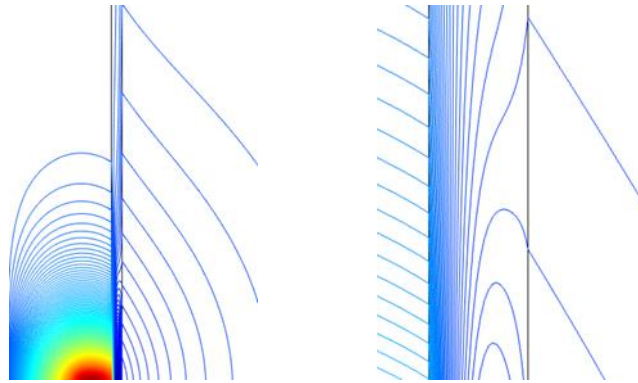


Fig.3 Magnetic line distribution Fig.4 Magnetic Valley local enlarged map

Can be seen from Figure 3, the magnetic lines in the pipe are mainly distributed in about twice the diameter of the region, the strongest magnetic field in the region. Within the wall of the tube, at a distance from the excitation coil, a small amount of magnetic field lines are substantially parallel to the tube wall and enter the far field. Figure 3 in the magnetic valley after a partial enlargement of Figure 4, we can see the existence of magnetic Valley, magnetic lines appeared roundabout. The magnetic field in the far field is mainly axial, and B_z is the axial component of magnetic induction. In the distance from the excitation coil 3 times at the far field magnetic field strength of the axial component B_z amplitude and phase along the diameter direction of the curve, shown in Figure 5,6.

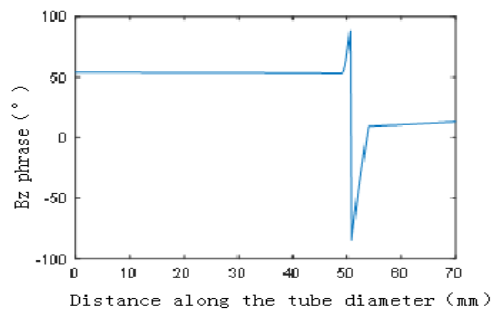


Fig.5 Bz Amplitude

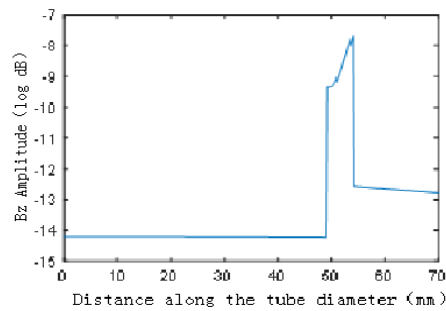


Fig.6 Bz Phrase

As can be seen from FIGS. 5 and 6, the amplitude and phase of the axial component B_z of the magnetic flux in the tube (0-49 mm) are substantially constant. Therefore, the detection of a certain point inside the coil B_z can completely represent the average coil cross-sectional area S_{Bz} .

The outer diameter of 108mm ferromagnetic steel pipe as the simulation and experimental research object. Detection of defects using multiple small coil array signal form, when the detection coil and the pipe axial parallel to the coil induction voltage U and the coil at a certain point of the axial magnetic flux density B_z has the following relationship:

$$U = -j\omega B_z S$$

When the detection coil cross-sectional area S and the number of turns ω determine, the output detection voltage signal U and B_z have the same trend, so you can use a detection coil B_z amplitude and phase changes to characterize the detection coil inductance voltage U amplitude and phase

changes. Because the amplitude and phase of B_z in each point inside the detection coil are basically the same, take the amplitude and phase change of B_z in the detection coil axis instead of analyzing the coil induced voltage U .

3.3 Simulation of far field eddy current defect signal

Four defects with the same width and different depths are set on the outer wall of the pipe wall simulation model 3 times the diameter of the excitation coil. The widths of the defects are 5 mm and the depths are 1 mm, 2 mm, 3 mm and 4 mm, respectively. Through the simulation, the curves of the axial component B_z amplitude and the distance from the excitation coil under different depth defects are obtained, as shown in Figs. 7 and 8. It can be seen that when the defect exists, the amplitude and phase of B_z near the defect have changed.

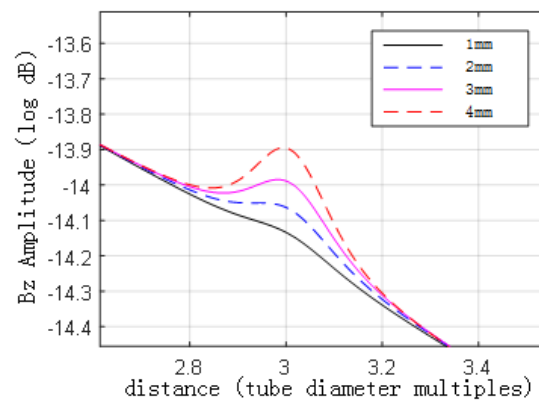


Fig.7 Different depth defects B_z amplitude

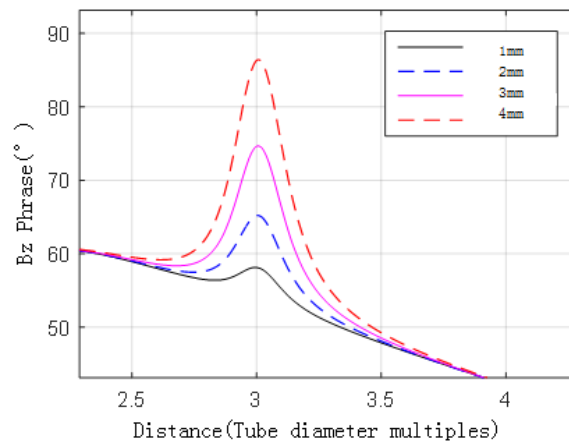


Fig.8 B_z phase with different depth defects

In order to quantitatively analyze the variation of the defect depth, the maximum value of the B_z phase protrusion at the defect center is extracted and the phase change at the corresponding depth defect is obtained by subtracting the phase at the defect-free location. The result is shown in Table 1.

Table 1. Change of B_z phase under different depth defects

defect(mm)	1	2	3	4
B_z The amount of phase change($^{\circ}$)	7.21	14.84	23.15	31.03

4. Experimental analysis of far field eddy current testing in pipeline

In the experiment, the ferromagnetic steel pipe with the same size as the simulation model (outer diameter 108mm, pipe wall thickness 5mm) was used. In the outer wall of the tube, three full circumferential groove defects with the same width and different depths were machined, with a width of 5 mm and depths of 1 mm, 2 mm and 3 mm, respectively. Far-field eddy current probe detection coil part of the array using a small coil differential form, the test results shown in Table 2.

Table2 Different depth defects injury signal amplitude / phase

Defect depth(mm)	Injury signal voltage amplitude(V)	Injury signal voltage phase(°)
1.0	0.79	27.67
2.0	1.55	52.11
3.0	2.10	73.82

Table 2 shows that as the defect depth increases, the magnitude of the injury signal voltage increases and the phase of the injury signal voltage also gradually increases. The depth of the defect is in direct proportion to the phase of the induced output voltage of the detection coil.

5. Conclusion

Through the simulation of the far-field eddy simulation model, the distribution of the magnetic field under a given excitation condition and the result that the amplitude and phase of the axial component B_z of the magnetic induction intensity in the far field are almost constant throughout the inner diameter of the tube are obtained. Through the simulation analysis And experimental verification, when the depth of the defect is different, the phase of the injury signal is also different, and the two shows a direct relationship between myopia.

References

- [1] Li Jiawei, Chen Jidui, etc. Nondestructive testing manual[M]. Beijing: Machinery Industry Press, 2002.
- [2] Sun Y S, Qu M X, Si J T, et al. Improvement in remote-field eddy current probe structure[J]. Ndt & E International, 1995, 28(4):249-249(1).
- [3] Huang Songling. Electromagnetic nondestructive testing of new technologies[M]. Beijing: Tsinghua University Press, 2014.
- [4] Kim D, Udpa L, Udpa S. Remote field eddy current testing for detection of stress corrosion cracks in gas transmission pipelines[J]. Materials Letters, 2004, 58(15):2102-2104.
- [5] Xiao Dan, Si Yibing, Huang Bo, etc. Finite Element Simulation of Pipeline Defects Identification Based on Far - Field Eddy Current Method [J]. Measurement and Control Technology, 2012, 31(5):131-135.
- [6] Lin Feiyu, Gen Yansheng, Wang Wenjun, etc. Simulation of Far Field Vortex Casing Testing[J]. Petroleum machinery, 2010, 38(9):19-21.